CRITICAL CONDITIONS FOR RILL INITIATION

C. Yao, T. Lei, W. J. Elliot, D. K. McCool, J. Zhao, S. Chen

ABSTRACT. *Quantifying critical conditions of rill formation can be useful for a better understanding of soil erosion processes. Current studies lack a consensus and related rationale on how to describe these conditions. This study was based on the concepts that (1) the shear stress available for erosion at any given point is a function of the runoff rate, the slope steepness, and hydraulic characteristics of the surface; (2) rill incision begins when overland flow shear stress exceeds soil critical shear stress; and (3) the distance from the top of the slope to the point where rills form can be measured and analyzed as length to rill initiation and decreases with increase in slope and rainfall intensity. These concepts were tested with a representative silty-clay soil from the Loess Plateau in northwestern China on a large sloping indoor plot (8 × 3 m), with five different slopes using simulated rainfall at three rainfall intensities. Values of several hydraulic parameters at rill initiation were determined from the experimental data. The results showed relationships among slope steepness, rainfall intensity, and location of rill initiation. It was found that slope was relatively more important than rainfall intensity in determining the location of rill initiation. Soil critical shear stress determined in this study ranged from 1.33 to 2.63 Pa, with an average of 1.94 Pa. Soil critical shear stress was inversely related to slope and was not influenced by rainfall intensity. The results of this study were comparable with those of previous investigators.*

Keywords. *Critical condition, Critical shear, Erosion, Hillslope, Rill initiation.*

Soil erosion is defined as "a process of detachment and transportation of soil material by erosive agents" (Ellison and Ellison, 1947; Elliot and Laflen, 1993). Where surface erosion rates are high, rill erosion is frequently the dominant process (Ellison and Ellison, 1947; Foster, 1982; Govers, 1990, 1992; Govers and Rauws, 1986; Nearing et al., 1989; Nearing et al., 1997). The rill formation process includes detachment, entrainment, and transport of soil particles driven by surface water flow. The velocity at the point of detachment is governed by the energy balance between that of the flowing water and that consumed by bed roughness and soil detachment, entrainment, and transport processes. Rills start to appear when the erosivity of the overland flow surpasses the resistance of the soil to detachment (Rauws and Govers, 1988), i.e., when there are sufficient forces available to detach and dislocate the particles. After the detachment and entrainment of the particles, the flowing water must have enough energy to transport these soil particles if a rill is to form. Detachment of the particles is a crucial step in soil surface erosion.

The critical conditions for rill formation have been the focus of many researchers. The idea of a rill formation threshold condition was first conceptualized by Horton (1945) and later by Schumm (1956), who respectively used the concepts of "the belt of no erosion" and "constant of channel maintenance" to describe the length of slope above the point of rill initiation. Ellison and Ellison (1947) and Schumm (1956) advanced understanding of the threshold conditions for incipient rilling and suggested that these conditions could be defined more quantitatively. The threshold for incipient rilling was defined by Kirkby (1978) as "when duration of runoff exceeds this point in time, rill processes will dominate over inter-rill processes and rill initiation may take place." Torri et al. (1987) set a criterion to define the rill formation as when an incised channel is at least 5 cm long, 0.5 cm deep, and 1 to 2 cm wide. Continuous development of the rill after its initiation depends upon the flow pattern and the morphological evolution of the rills. Rill pattern and evolution are not independent (Nearing et al., 1991a). During the rill formation process, incised rill channels are formed as the result of detachment and transport of soil particles by the flowing water. Such channels function as both sediment source areas and sediment transport conduits on hills. Numerous studies have been conducted to explore the mechanisms of the rill formation process. Most of these studies, however, are related to rill development after incision (Lyle and Smerdon, 1965; Moss et al., 1980; Foster, 1982; Rose, 1985; Govers and Rauws, 1986; Elliot, 1988; Nearing et al., 1989, 1991a, 1991b; Morgan et al., 1992; Shainberg et al., 1994; Morgan, 1995; Nearing et al., 1997). Few studies have focused on slope steepness and how it affects rill formation. Foster (1975) carried out a study

Submitted for review in June 2007 as manuscript number SW 7056; approved for publication by the Soil & Water Division of ASABE in October 2007.

The authors are **Chunmei Yao,** Research Assistant, College of Hydraulic and Civil Engineering, China Agricultural University, Beijing, China, and Department of Biological Systems Engineering Department, Washington State University. Pullman, Washington; **Tingwu Lei, ASABE Member Engineer,** Professor, College of Hydraulic and Civil Engineering, China Agricultural University, Beijing, China; **William J. Elliot, ASABE Member Engineer,** Professor and Project Leader, Soil and Water Engineering, USDA Forest Service, Rocky Mountain Research Station. Moscow, Idaho; **Donald K. McCool, ASABE Fellow,** Research Leader, USDA-ARS Pacific West Area, Washington State University, Pullman, Washington; **Jun Zhao,** Senior Engineer, State Key Laboratory of Soil Erosion and Dryland Farming on the Loess Plateau, Institute of Soil and Water Conservation, Chinese Academy of Sciences and Ministry of Water Resources, Yangling, China; and **Shulin Chen, ASABE Member Engineer,** Professor, Department of Biological Systems Engineering, Washington State University, Pullman, Washington. **Corresponding author:** Shulin Chen, Department of Biological Systems Engineering, Washington State University, Pullman, WA 99164-6120; phone: 1-509-335-3743; fax: 1-509-335-2722; e-mail: chens@wsu.edu.

 © 2008 American Society of Agricultural and Biological Engineers ISSN 0001–2351

relating shear on an eroding rill to slope steepness and discharge, but did not include erosion in the study. Elliot et al. (1990) found that slope steepness was associated with critical shear for rill formation, but the study had only a single slope for a given soil, so they were unable to determine if differences in critical shear were due to soil properties or to the hydraulic properties of the runoff.

Better understanding is needed for determining the critical conditions for rill formation. Most of the previously reported research on rill formation was performed on small plots, and the erosion process was observed for a single rill. Studies with larger plots that allow for observations with groups of rills may lead to more generalized conclusions as to how and under what conditions rills initially form on a hillslope. The purpose of this study was to better understand the process of rill formation. This study was based on the concept that: (1) the shear stress available for erosion at any given point is a function of the runoff rate, the slope steepness, and hydraulic characteristics of the surface; (2) rill incision begins when overland flow reaches and exceeds soil critical shear stress; and (3) the distance from the top of the slope to the point where rills form can be measured and analyzed and decreases with increase in slope and rainfall intensity. To verify these concepts, a study was carried out using a large indoor tilting runoff plot with simulated rainfall.

Material and Methods

Experimental Setup

The experiment was conducted in the Key Laboratory of Soil Erosion and Dry Land Farming on the Loess Plateau, Institute of Soil and Water Conservation, Chinese Academy of Sciences, Yangling, Shaanxi, China. A large runoff plot (8 × 3 m) was used with a rainfall simulator (fig. 1). The plot rested on a platform that was adjustable for slopes ranging from 0% to 57.7%. Rulers were fixed on the metal borders of the plot, and the entire plot surface was divided into 24 blocks (1 m^2 each) using fine thread suspended about 5 cm over the plot in order to aid in measuring the position of rill initiation during the experiment.

The plot was initially prepared in a horizontal position. A 20 cm layer of sand was uniformly placed in the bottom of the plot box; drainage holes in the bottom provided free drainage. On the top of the sand layer, a silty-clay (loess) soil was packed loosely and evenly to a depth of 30 cm. The soil texture was 8% clay (<0.002 mm), 68% silt (0.002 to 0.05 mm), and 24% sand (0.05 to 2 mm) as defined by the USDA classification system. The soil was obtained from the root layer (top 50 cm) of a cultivated field located in the Loess Plateau area in northwestern China. After being transported from the field to the experimental site, the soil was air-dried and crushed. The clods in the soil were broken up, and the soil was sieved with a 10 mm screen. The soil was packed in the plot to a bulk density of 1.15 g cm^{-3}. During the packing process, a static weight method was used to pack the soil uniformly in the box. After packing, the soil surface was smoothed manually with a rake. Following the soil preparation, simulated rainfall was applied for 30 min at 30 mm h^{-1} intensity. After the initial rainfall, the packed soil was saturated and allowed to equilibrate for at least 24 h while the plot remained in a horizontal position to ensure a uniform and homogeneous initial soil moisture profile.

Figure 1. Indoor flume at the start of a typical simulation.

The rainfall simulation system provided rainfall intensities ranging from 25 to 200 mm h^{-1} over an effective simulation area of 13 × 15 m. The nozzle height of 18 m ensured that the raindrops would reach terminal velocity on the highest point of the plot. Whenever the rainfall intensity was changed, the new intensity was verified with 42 rain gauges distributed evenly within the rainfall simulation area. Uniformity of rainfall intensity was considered acceptable when 90% of the rain gauge measurements were within ±3% of the targeted rainfall intensity.

Treatments

The treatments included five slopes (8.75%, 17.63%, 26.79%, 36.40%, and 46.63%), each with three levels of rainfall intensity (50, 100, and 150 mm h^{-1}), for a total of 15 treatments (table 1). These ranges for the slope and rainfall intensity were selected to cover the storm and field conditions observed in the Loess Plateau Area.

Table1. Slope steepness values and rainfall intensities for each test number.

Rain Intensity (mm h^{-1})	Slope				
	5° (8.75%)	10° (17.36%)	15° (26.79%)	20° (36.40%)	25° (46.63%)
50	1	2	3	4	5
100	6	7	8	9	10
150	11	12	13	14	15

Experimental Procedure

Each test was conducted 24 h after the initial rainfall and prewetting following the soil preparation. The starting time of the simulated rainfall, the time when runoff reached the outlet of the plot, and the time when rill initiation occurred were recorded. In each experiment, sediment samples together with runoff were taken every minute for about 1 h after the start of runoff. Discharge was measured every minute by collecting the runoff from the outlet gutter at the lower end of the plot (fig. 1) with a bucket. Runoff volumes were determined by weighing each bucket. To separate the suspended sediments from water in the samples, the buckets containing the runoff samples were allowed to settle overnight. The buckets were weighed before and after decanting the water. The remaining water and sediment were transferred into containers that were dried in ovens at 105°C for at least 24 h, or until the samples were completely dry. The mass of the sediment was then measured and used to calculate sediment concentration.

Flow velocity was measured visually with a dye-tracing technique (potassium permanganate) using a stopwatch to record the time required for the dye to travel a given distance (Nearing, 1991; Nearing et al., 1997; McIsaac et al., 1992). A modification to the technique was made to facilitate measurement of the local velocity in addition to the average velocity along the entire plot. When a rill appeared, the position of the rill incision was recorded. A 0.5 m ruler was then positioned so that the middle point of the ruler matched the incision point. The dye was applied at the upslope end of the hand-held ruler; and the time taken for the dye to travel the entire ruler length was recorded. This method was used to estimate the velocity where each rill appeared. Several measurements were made for each rill, and average values of all rills were used in the analysis. At the same time, the distance from the top of the plot to the point of initiation was measured; the median distance of all rills in a test was used in subsequent calculations as length to rill initiation. Other observations made during and after the experiments included photographing the rill formation pattern and video-recording the change in rill morphology.

Data Analysis

Terminology for Analyses

The critical point of rill incision is a small pit that appears on the plot during the test and that later develops into a rill. The critical conditions of rill incision should be related to hydraulic parameters of the surface water flow. When the overland flow reaches a critical point, the point at which the soil particles lose the ability to remain in place and are detached by the flowing water, a rill starts to form. Two important hydraulic parameters of the flowing water at rill initiation may be the shear stress and velocity. At the point of rill initiation, the values of these two parameters can be defined as τ_i and V_i, respectively. Soil critical shear stress (τ_c) is a soil property that can be estimated by assuming it is the same as the shear stress (τ_i) of the overland flow at the point of rill initiation. In reality, the shear stress (τ_i) of flowing water at the point of rill initiation is greater than but very close to soil critical shear stress (τ_c) because soil detachment has already occurred when the values related to the rill initiation are measured in the experimental run. In this article, τ_i refers to the shear stress of the flow, τ_c refers to soil critical shear, and they have the same values for a given test. Slope length to rill initiation (L_i) is defined as the distance from the top of the plot to the point where a rill began to form.

Soil Critical Shear Analysis

Figure 2 shows the basis for the development of the critical shear analysis using the following equations. For near-steady state conditions, unit overland flow discharge (q) at a horizontal distance (x) from the divide (top of plot) can be calculated from equation 1 (Bryan, 1989):

$$q(x) = Rx \tag{1}$$

R (runoff) is defined as:

$$R = P - I \tag{2}$$

where P is the rainfall rate, and I is the mean infiltration rate. Combining equations 1 and 2 and accounting for the slope of the plot leads to:

$$q(l) = (P - I)l \cos \alpha \tag{3}$$

where α is the slope angle, and l is the distance from the top to any point on the hillslope. Assuming that the runoff rate has a linear distribution with distance down the plot, as shown in equations 1 and 3, leads to:

$$q_i = \frac{L_i}{L} \times q \tag{4}$$

where q_i is the unit flow discharge at the point of rill initiation, L_i is the distance from the top to the point of rill initiation on the hillslope, L is the plot length (8 m), and q is the observed plot runoff. The continuity equation for a unit flow width is:

$$h_i = \frac{q_i}{v_i} \tag{5}$$

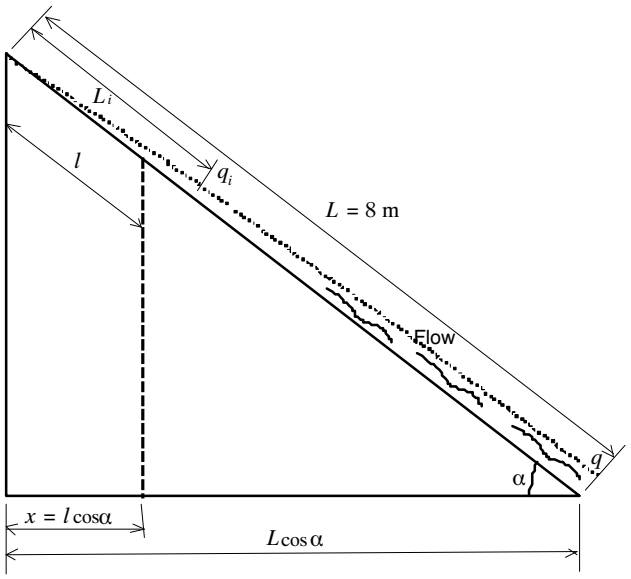

Figure 2. Discharge and slope length relationship of the flowing water on a hillslope.

where h_i is the mean depth of flow at the point of rill initiation, q_i is the unit flow at rill initiation (calculated from eq. 4), and v_i is the velocity measured at the point of rill initiation.

Flow depth (h_i) at rill initiation is derived by solving equation 5. Depth h_i can be used to determine the hydraulic shear at the point of rill initiation from equation 6:

$$\tau_c = \tau_i = \rho g h_i S \quad (6)$$

Results and Discussion

Rill Formation Pattern

Figure 3 shows multiple rills formed in each experimental run. In this figure, all pictures in the same row had the same rainfall intensity. The three rows in top to bottom sequence represent three different rainfall intensities: 50, 100, and 150 mm h^{-1}, respectively. Similarly, all pictures in the same column had the same slope. Consequently, the five columns

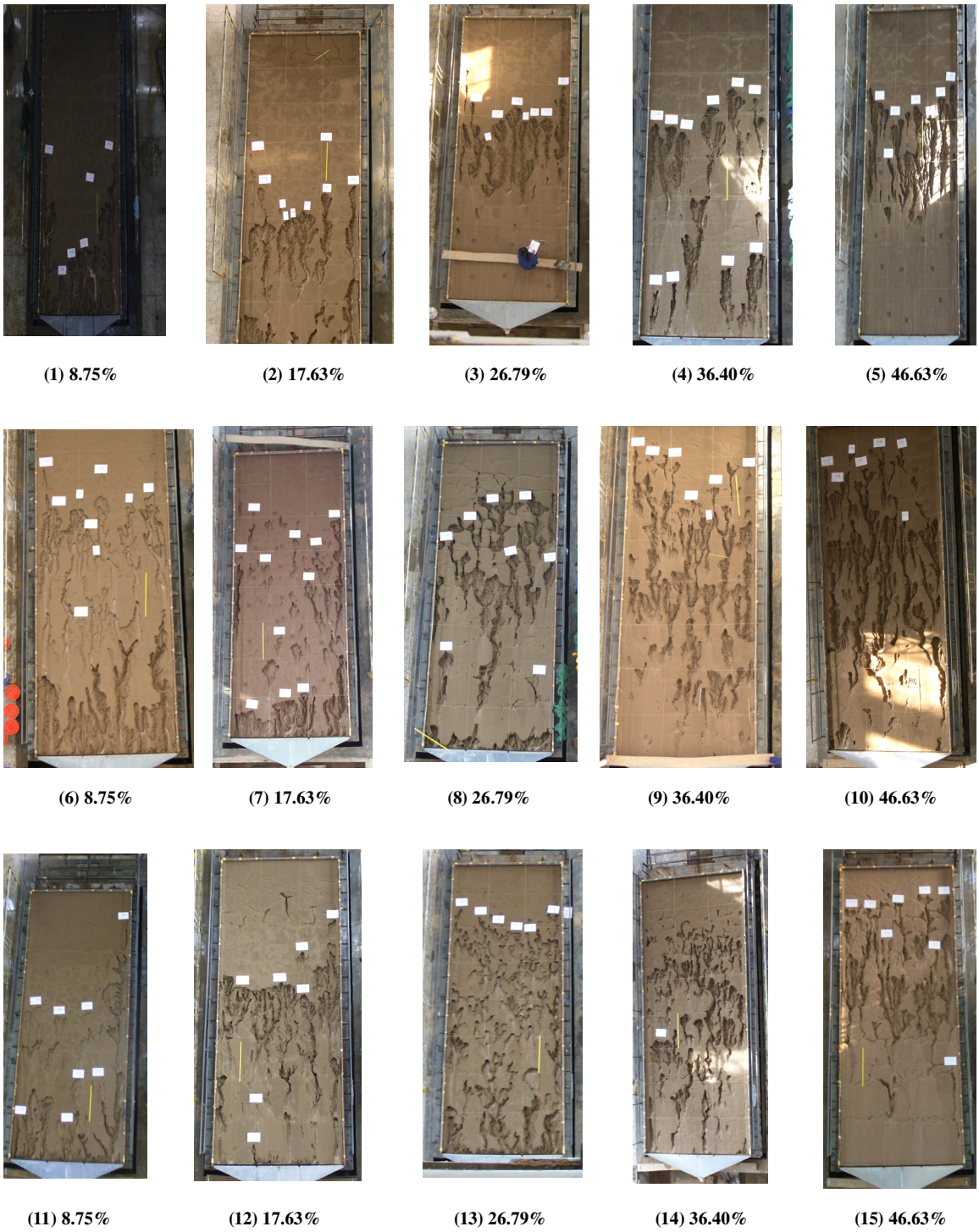

Figure 3. View of rill development under different slopes under different rainfall intensity (refer to table 1). Rainfall rate, top to bottom: 50, 100, and 150 mm h^{-1}. Plot slope, left to right: 8.75%, 17.63%, 26.79%, 36.40%, and 46.63%.

represent five different slopes: 8.75%, 17.63%, 26.79%, 36.40%, and 46.63%, respectively. During the experiment, when a rill initiation point was observed, the distance from the top of the plot to the point of initiation was measured. The average of all the observations for a given experiment was calculated as slope length to rill initiation. It can be seen from figure 3 that, as a general trend, when the slope increased (from left to right in the same row), the slope length to rill initiation decreased. The same trend can be observed as the rainfall intensity increased (from top to bottom in the same column). Figure 3 also shows that the rills in the same test had similar slope lengths to initiation. It should be noted that the upper ends of the rills in the pictures were not the exact position of rill initiation during the experiment due to headcutting that occurred following rill formation. However, these positions shown in the picture provide an illustration of the variability associated with rill formation. During each test, the surface runoff that was available to initiate rill formation at the upstream end of the rills was limited, so the upward movement of rill headcut from the rill incision point was not significant compared with the development of the rills downslope of the point of rill initiation.

Velocity at Rill Initiation

Table 2 shows the slope lengths, flow rates, velocities, and depths at the points of rill initiation. Figure 4 shows the relationship between velocity at rill initiation and slope steepness. The velocity, measured as an average at the point of rill incision, increased with increasing slope. In table 2 and figure 4, the average velocities were observed as almost the same at the point of rill initiation under different rainfall intensities for the same slope. As shown in table 2, the measured average velocity at rill initiation ranged from 3.2 to 5.2 cm s^{-1}.

Slope Length to Rill Initiation

Slope length to rill initiation (L_i) values are presented in table 2 and figure 5. Once soil critical shear was exceeded, rills developed. Figure 5 shows that slope length to initation decreased with increasing slope, as well as with increasing rainfall intensity. The results are summarized graphically in figure 6, in which the positions of rill initiation at different rainfall intensities are described by a series of lines connecting various slopes. In figure 6, each dashed line that crosses a slope line represents a rill incision point. The numbers with each point correspond to the test numbers presented in table 1. Figure 6 illustrates how the slope length (L_i) was affected by rainfall intensity and slope steepness.

Table 2. Experimental data at point of rill initiation.

Rainfall Intensity, I (mm h^{-1})	Slope, S (%)	Slope Length to Rill Initiation L_i (m)	Unit Flow Rate, q_i (m^2 s^{-1} 10^{-4})	Flow Velocity, V_i (cm s^{-1})	Depth of Flow, h_i (m 10^{-3})	Critical Shear Stress, τ_c (Pa)
50	8.75	6.81	1.0139	3.3	3.073	2.633
	17.63	4.62	0.5479	4.2	1.304	2.253
	26.79	3.50	0.3352	4.7	0.713	1.872
	36.40	2.90	0.2465	5.1	0.483	1.723
	46.63	2.40	0.1700	5.2	0.327	1.493
100	8.75	6.30	0.9781	3.3	2.964	2.540
	17.63	4.17	0.4878	3.9	1.251	2.160
	26.79	2.91	0.3651	4.4	0.830	2.178
	36.40	2.40	0.2363	4.8	0.492	1.755
	46.63	2.11	0.1607	5.2	0.309	1.411
150	8.75	5.50	0.9716	3.2	3.036	2.602
	17.63	3.57	0.4831	4.1	1.178	2.035
	26.79	2.71	0.2998	4.4	0.681	1.788
	36.40	2.29	0.1865	4.9	0.381	1.357
	46.63	1.93	0.1460	5.0	0.292	1.334
Average				4.4		1.942

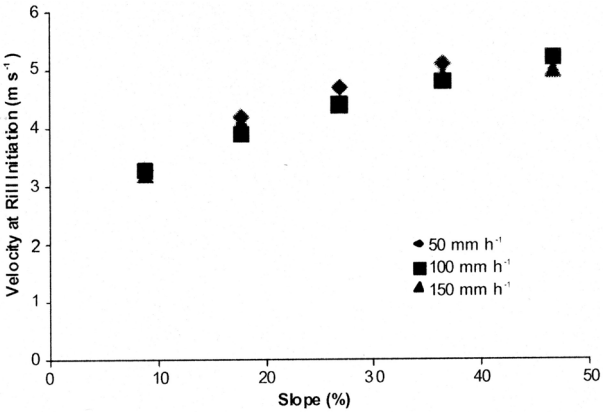

Figure 4. Relationship of velocity at rill initiation and slope.

Change Rate of L_i in Response to Steepness and Runoff Rate

It may be useful to determine what is more sensitive in soil erosion: slope steepness or rainfall intensity. Figure 6 showed intuitively and table 2 showed quantitatively that the degree of change in slope length to rill initiation was different between slope and rainfall intensity, and that the change rate due to the slope was more than that due to rainfall intensity within the range of this experiment. This can be more clearly demonstrated using the relative change rate, defined as:

$$r = \frac{\Delta L_i}{L_0} \times 100\% \quad (7)$$

where r is the change rate (%) of slope length to rill initiation, ΔL_i is the change range of slope length to initiation (from 8.75% to 46.63% slope in different rainfall intensities or from 50 to 150 mm h^{-1} rainfall intensity in different slopes), and L_0 is slope length to rill initiation of 8.75% slope in different rainfall intensities or that of 50 mm h^{-1} rainfall intensity in

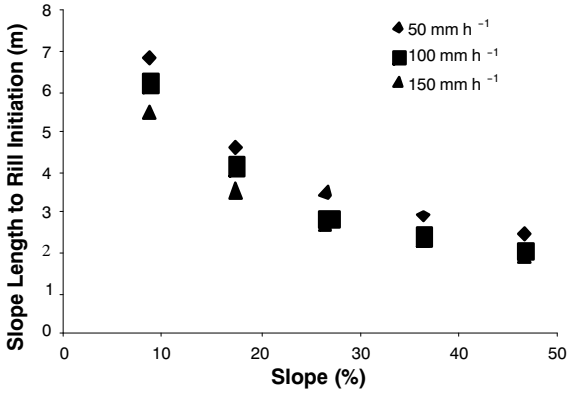

Figure 5. Relationship of slope length to rill initiation and slope.

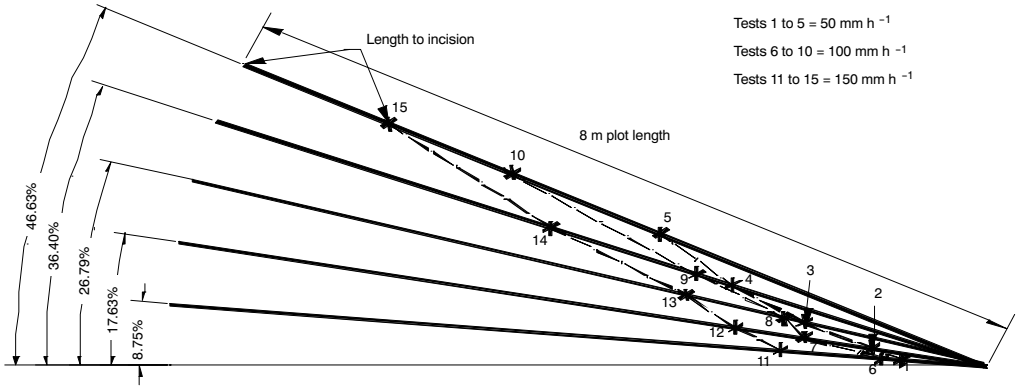

Figure 6. Slope length to rill initiation for different rainfall intensities with different plot slopes.

different slopes. The results from this sensitivity analysis are given in table 3. The slope length to rill initiation has a greater sensitivity to slope than to rainfall intensity. The results in table 3 show that the impact of slope steepness on slope length to rill iniation (L_i) is more significant than that of rainfall intensity: 65.7% versus 21.2% within the range tested.

Soil Critical Shear Stress

Table 2 presents the slope length to rill initiation, flow depth, and soil critical shear for each test. The results indicated that in this study the soil critical shear stress ranged from 1.33 to 2.63 Pa, with an average of 1.94 Pa. Table 2 and figure 7 show that values of soil critical shear stress were lower for the steeper slopes. A trend line added to figure 7 for the 50 mm h^{-1} rainfall indicates a high correlation. Figure 7 indicates that gravitational forces may be contributing to rill formation as well as the hydraulic force for steeper slopes. The observed hydraulic shear at the lower slope better estimates the soil critical shear than the values at steeper slopes because of the influence of gravitational forces. These results can be compared to results found by others on silt loam soils. Two of the 30 soil types studied by Laflen et al. (1991) had similar texture to the soil used in this study. These two types of soil were Nansene (from Whitman County, Washington; 20.1% sand, 68.8% silt, and 11.1% clay) and Portneuf (from Twin Falls, Idaho; 21.5% sand, 67.4% silt, and 11.1% clay), respectively. Laflen et al. (1991) calculated the critical shear values on these soils to be 3.05 and 3.11 Pa, respectively. Using a different method of analysis, Gilley et al. (1993) determined that the soil shear stress values for the two soils were 3.58 and 4.30 Pa, respectively. The steepness of the plots in the studies of Laflen et al. (1991) and Gilley et al. (1993) were only 6.10% and 5.57%, respectively. The values of critical shear in table 2 for the 8.75% plot slope ranged from 2.54 to 2.63 Pa, similar to the values found by Laflen et al. (1991) and Gilley et al. (1993). This decrease in critical shear with slope is different from the results of Elliot et al. (1990), who found that soil formed on steeper slopes

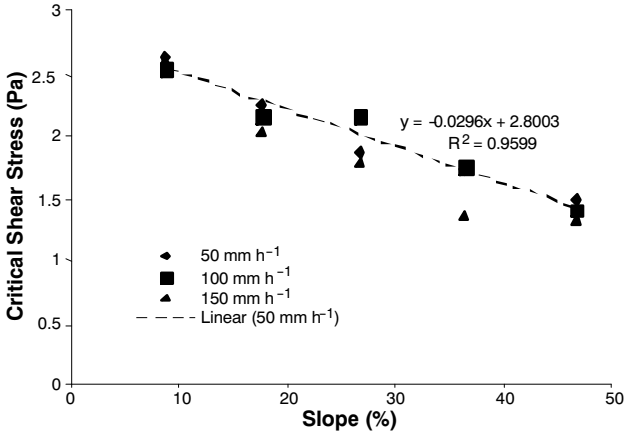

Figure 7. Relationship of critical flow shear stress, slope, and rainfall intensity.

tended to exhibit higher critical shear values. In this study, however, the same soil was used for all slopes.

Comparison with Other Reports

The results of this study are comparable with some other investigations conducted under various conditions. Table 4 summarizes the comparisons in terms of experimental setup, critical shear stress, and flow velocity. Despite differences in soil type, plot size, and methodologies, the critical shear stress values obtained in this study were either within the range of that of the other reports, or in the same order of magnitude. For example, Laflen et al. (1991) studied 56 soil types and reported a shear stress range from 0.00 to 6.64 Pa. Gilley et al. (1993) studied 30 soil types and used the same data set as Laflen et al. (1991) but a different calculation method and obtained a shear stress range from 1.73 to 10.60 Pa. These values were consistent with the results of this study (1.33 to 2.63 Pa). Few of the studies reported flow velocity. Large discrepancies existed among those that did report flow velocity. Nearing (1991) used Russell silt loam soil with rill

Table 3. Slope length at rill initiation (L_c) change rate with slope and rainfall intensity change.

Factor	Slope Change (8.75% to 46.63%)			Rainfall Intensity (50 to 150 mm h^{-1})				
Level	50	100	150	8.75%	17.63%	26.79%	36.40%	46.63%
L_i change range	6.81 to 2.40	6.30 to 2.11	5.50 to 1.93	6.81 to 5.50	4.62 to 3.57	3.50 to 2.71	2.90 to 2.29	2.40 to 1.93
L_i change rate (%)	65	67	65	19	23	23	21	20
L_i average change rate	65.7%			21.2%				

Table 4. Comparison with other results.

Author (year)	Plot Size	Soil	Flow Velocity (cm s^{-1})	Critical Shear Stress (Pa)
Nearing (1991)	9 m long, 1 m wide	Russell silt loam	50 to 100	0.49 to 1.96
Laflen et al. (1991)	9 m long, 0.46 m wide	56 kinds of soils	20 to 50	0 to 6.64, Nansene: 3.05
Govers (1992)	12 m long (6 m effectively), 0.117 m wide	Five well-sorted quartz materials		0.20 to 0.35
Gilley et al. (1993)	9 m long, 0.46 m wide	30 kinds of soils	20 to 50	1.73 to 10.60, Nansene: 3.58
Shainberg et al. (1994)	0.5 m long, 0.046 m wide, and 0.12 m deep	Miami silt loam		0.48 to 4.80 Average: 3.32
Flanagan and Livingston (1995)		Soils <30% sand		3.50
Shainberg et al. (1996)	0.5 m long, 0.046 m wide, and 0.12 m deep	Israel's three main arable soil types		0.79 to 1.72 Average: 3.32 1.33
Wu (1997)	1 m long, 0.4 m wide	Silty loess soil from the Loess Plateau	5.82 to 15.86	
Van Klaveren and McCool (1998)	2.73 m long, 0.46 m wide	Palouse soil		Under freeze-thaw conditions: 2.40
Mancilla (2004)	Field single rill	Palouse soil		Unfrozen: 0.33-3.60 One freeze-thaw cycle: 0.66 to 1.65
Govers (1985) and Govers and Rauws (1986)			Critical shear velocities: 3 to 3.5	
Persyn et al. (2005)	4 m long	Biosolids, yard waste, bio-industrial, subsoil and top soil		4.50 to 13.00 (vegetated) 2.70 to 9.80 (unvegetated)
Our experiment	8 m long, 3 m wide	Silty loess soil from the Loess Plateau	Flow velocity at rill initiation: 3.4 to 5.0	Critical flow shear stress: 1.33 to 2.63 Average: 1.92

flow velocities of 50.00 to 100.00 cm s^{-1}; Wu (1997), using a silty-clay (loess) soil similar to that used in this study but with different texture, determined rill flow velocity as 5.0 to 16.0 cm s^{-1}. The flow velocities in the Gilley et al. (1993) and Laflen et al. (1991) studies were 20 to 50 cm s^{-1}, with a velocity at rill initiation of less than 20 cm s^{-1} in the rills (Elliot et al., 1989). The rill flow velocities in the above three studies were rill velocity measured after rill development. In this study, flow velocity at rill initiation was determined as 3.4 to 5.0 cm s^{-1}, which was measured on overland sheet flow when rill incision appeared. Typically, after rill formation, the rill flow concentrated more, leading to a rill flow velocity that was higher than that of sheet flow under critical condition.

Conclusions

The following conclusions can be drawn from this study:

- Rainfall intensity and slope steepness both affected the distance from the top of the plot to the point of rill initiation, and the velocity at rill initiation.
- The slope length to rill initiation observed in the study ranged from 1.93 to 6.81 m. The value had a decreasing trend with respect to slope and rainfall intensity. The impact of slope on slope length to rill initiation was more significant than that of rainfall intensity.
- The average measured flow velocity at rill initiation ranged from 3.2 to 5.2 cm s^{-1}.
- Soil critical shear stress determined in this study for a silty-clay soil ranged from 1.33 to 2.63 Pa, with an average of 1.94 Pa.
- Soil critical shear stress varied inversely with slope, lilely as the influence of gravitational forces at steeper slopes.
- The results of this study were comparable with those of previous investigators.

More research is needed to better understand the force and energy involved in soil particle detachment, entrainment, and transport during the rill formation process.

Acknowledgements

This study was funded by the Natural Science Foundation of China under Project No. 40635027 for the experimental work. Partial support was provided by the Agricultural Research Center at Washington State University for data processing. We also thank the Water Conservation State Key Laboratory for Soil Erosion and Dry Land Farming on the Loess Plateau, Chinese Academy of Sciences, Ministry of Water Resources, for providing the test facility.

REFERENCES

Bryan, R. B. 1989. Laboratory experiment on the influence of slope length on runoff, percolation, and rill development. *Earth Surface Processes and Landforms* 14(3): 211-231.

Ellison, W. D., and O. T. Ellison. 1947. Soil erosion studies: Part VI. Soil detachment by surface flow. *Agric. Eng.* 28(9): 402-406.

Elliot, W. J. 1988. A process based rill erosion model. Unpublished PhD diss. Ames, Iowa: Iowa State University, Department of Agricultural Engineering.

Elliot, W. J., and J. M. Laflen. 1993. A process-based rill erosion model. *Trans. ASAE* 36(1): 65-72.

Elliot, W. J., A. M. Liebenow, J. M. Laflen, and K. D. Kohl. 1989. A compendium of soil erodibility data from WEPP cropland soil field erodibility experiments, 1987 and 1988. NSERL Report No. 3. West Lafayette, Ind.: USDA Agricultural Research Service.

Elliot, W. J., L. J. Olivieri, J. M. Laflen, and K. D. Kohl. 1990. Predicting soil erodibility from soil properties including classification, mineralogy, climate, and topography. ASAE Paper No. 902557. St. Joseph, Mich.: ASAE.

Flanagan, D. C., and S. J. Livingston. 1995. WEPP user summary: USDA Water Erosion Prediction Project (WEPP). NSERL Report No. 11. West Lafayette, Ind.: USDA Agricultural Research Service.

Foster, G. R. 1975. Hydraulics of flow in a rill. Unpublished PhD diss. West Lafayette, Ind.: Purdue University.

Foster, G. R. 1982. Modeling the erosion process. In *Hydrologic Modeling of Small Watersheds*, 297-360. C. T. Haan, ed. ASAE Monograph No. 5. St. Joseph, Mich.: ASAE.

Gilley, J. E., W. J. Elliot, J. M. Laflen, and J. R. Simanton. 1993. Critical shear stress and critical flow rates for initiation of rilling. *J. Hydrol.* 142: 251-271.

Govers, G. 1985. Selectivity and transport capacity of thin flows in relation to rill erosion. *Catena* 12(1): 35-49.

Govers, G. 1990. Empirical relationships for the transport capacity of overland flow. In *Erosion, Transport, and Deposition Process*, 45-63. IAHS Pub. No. 189. Wallingford, U.K.: IAHS Press.

Govers, G. 1992. Relationship between discharge, velocity, and flow area for rills eroding loose, non-layered materials. *Earth Surface Processes and Landforms* 17(5): 515-528.

Govers, G., and G. Rauws. 1986. Transporting capacity of overland flow on plane and on irregular beds. *Earth Surface Processes and Landforms* 11(5): 515-524.

Horton, R. E. 1945. Erosional development of streams and their drainage basins: Hydrophysical approach to quantitative morphology. *Bull. Geol. Soc. America* 56(3): 275-370.

Kirkby, M. J. 1978. *Hillslope Hydrology.* New York, N.Y.: Wiley-Interscience.

Laflen, J. M., W. J. Elliot, R. Simanton, C. S. Holzhey, and K. D. Kohl. 1991. WEPP soil erodibility experiments for rangeland and cropland soils. *J. Soil and Water Cons.* 46(1): 39-44.

Lyle, W. M., and E. T. Smerdon. 1965. Relation of compaction and other soil properties to erosion resistance of soils. *Trans. ASAE* 8(3): 419-422.

Mancilla, G. 2004. Critical shear stress and rill sediment transport capacity of Palouse soil. Unpublished PhD diss. Pullman, Wash.: Washington State University, Department of Agricultural Engineering.

McIsaac, C. F., J. K. Mitchell, J. W. Hummel, and W. J. Elliot. 1992. An evaluation of unit stream power theory for estimating soil detachment and sediment discharge from tilled soils. *Trans. ASAE* 35(2): 535-544.

Morgan, R. P. C. 1995. The European Soil Erosion Model: An update on its structure and research base. In *Conserving Soil Resources, European Perspectives*, 286-299. R. J. Rickson, ed. Oxon, U.K.: CAB International.

Morgan, R. P. C., J. N. Quinton, and R. J. Rickson. 1992. *EUROSEM Documentation Manual.* Silsoe, Bedford, U.K.: Silsoe College.

Moss, A. J., P. H. Walker, and J. Hutka. 1980. Movement of loose sandy detritus by shallow water flows: An experiment study. *Sediment. Ged.* 25(1-2): 43-66.

Nearing, M. A. 1991. A probabilistic model of soil detachment by shallow turbulent flow. *Trans. ASAE* 34(1): 81-85.

Nearing, M. A., G. R. Foster, L. J. Lane, and S. C. Finkner. 1989. A process-based soil erosion model for USDA Water Erosion Prediction Project technology. *Trans. ASAE* 32(5): 1587-1593.

Nearing, M. A., J. M. Bradford, and S. C. Parker. 1991a. Soil detachment by shallow flow at low slope. *SSSA J.* 55(2): 339-344.

Nearing, M. A., S. C. Parker, J. M. Bradford, and W. J. Elliot. 1991b. Tensile strength of thirty-three saturated repacked soils. *SSSA J.* 55(6): 1546-1551.

Nearing, M. A., L. D. Norton, and D. A. Bulgakov. 1997. Hydraulics and erosion in eroding rills. *Water Resources Res.* 33(4): 865-876.

Persyn, R. A., T. D. Glanville, T. L. Richard, J. M. Laflen, and P. M. Dixon. 2005. Environmental effects of applying composted organics to new highway embankments: Part III. Rill erosion. *Trans. ASAE* 48(5): 1765-1772.

Rauws, G., and G. Govers. 1988. Hydraulic and soil mechanical aspects of rill generation on agricultural soils. *J. Soil Sci.* 39(1): 111-124.

Rose, C. W. 1985. Development in erosion and deposition models. *Advances in Soil Sci.* 2: 1-63.

Schumm, R. A. 1956. Evolution of drainage systems and slopes in badlands at Perth Amboy, New Jersey. *Bull. Geol. Soc. America* 67(5): 597-646.

Shainberg, I., J. M. Laflen, J. M. Bradford, and L. D. Norton. 1994. Hydraulic flow and water quality characteristics in rill erosion. *SSSA J.* 58(4): 1007-1012.

Shainberg, I., D. Goldstein, and G. J. Levy. 1996. Rill erosion dependence on soil water content, aging, and temperature. *SSSA J.* 60(3): 916-922.

Torri, D., M. Sfalaga, and M. Del Sette. 1987. Splash detachment: Runoff depth and soil cohesion. *Catena* 14(1-3): 149-155.

Van Klaveren, R. W., and D. K. McCool. 1998. Erodibility and critical shear of a previously frozen soil. *Trans. ASAE* 41(5): 1315-1321.

Wu, P. 1997. The dynamics of water erosion experiment research (in Chinese). *Shaanxi Science and Tech. Press* (China), 17-20.